

Gradient Based Quantum Optimal Control in a Chopped Basis

J. J. W. H. Sørensen, M. O. Aramburu, T. Heinzl, and J. F. Sherson
*Aarhus University**

(Dated: December 14, 2024)

We propose a quantum optimal control algorithm that performs a gradient descent in a reduced basis named GRAdient Optimization Using Parametrization (GROUP). We compare this optimization algorithm to the other state-of-the-art algorithms in quantum control namely, Gradient-Ascent Pulse Engineering (GRAPE), Krotov's method and Nelder-Mead using Chopped Random Basis (CRAB). We find that GROUP converges much faster than Nelder-Mead with CRAB and achieves better results than GRAPE and Krotov's method on the control problem presented here.

I. INTRODUCTION

Technological advances in the experimental toolbox in physical chemistry and atomic, molecular, and optical (AMO) physics currently enable exciting new developments in the manipulation of complex quantum systems. Gradually, the focus is shifting from verifying the validity of theoretical models towards controlling and manipulating quantum systems for specific technological applications [1, 2]. Some examples of this trend are quantum state preparation [3, 4], atomic clocks [5], quantum based sensors [6–8], quantum simulators [9], and quantum computers [10, 11].

These applications require the ability to steer the quantum dynamics precisely using external control fields. The desired dynamics are typically encoded in terms of an expectation value for some operator using a functional. This can e.g. be some target state [12], a unitary gate operator [13], or an experimental signal [14]. Quantum Optimal Control (QOC) is a framework that enables the design of control strategies that achieve the desired dynamics [15–17]. QOC has been studied in a wide range of physical systems [12, 18–20]. Central in QOC are local optimization algorithms that maximize or minimize the functional. These methods can be extended with global optimization methods [21]. These local algorithms can broadly be divided along two axes [21]. The first axis is derivative-based versus derivative-free algorithms and the second is optimization in full or reduced dimensions. Derivative-free algorithms only evaluate the cost functional. A central example is the Nelder-Mead algorithm typically used in combination with a Chopped RAndom Basis (CRAB) [20, 22]. On the other hand, derivative-based methods use both the functional and derivative information. Important examples from QOC are the GRAdient-Ascent Pulse Engineering (GRAPE) and Krotov's method [23–25]. Reduced basis methods parametrize the control in some basis of smooth functions [20]. This removes redundant dimensions and eases the search for optimal solutions. However, a too low dimension can introduce artificial traps since the parametrization is no longer able to ade-

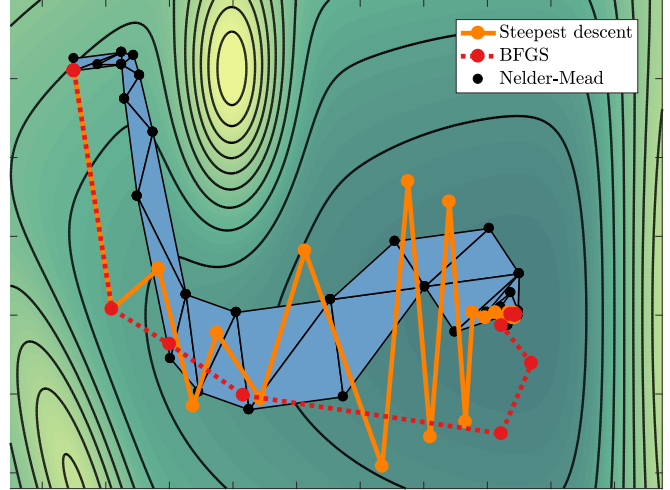


FIG. 1. Comparison of gradient-based and gradient free optimization methods in an artificial landscape. The shaded blue triangles show the gradient free method Nelder-Mead. The solid orange line and the dotted red line are gradient based algorithms steepest descent and BFGS respectively. Steepest descent exhibits the characteristic zig-zag type behavior, which BFGS avoids due to the inverse Hessian approximation. Nelder-Mead, steepest descent and BFGS respectively use 45, 34 and 15 iterations for convergence.

quately describe the optimal solutions [26]. Ideally, one should combine both these two approaches and perform derivative-based optimization in a reduced basis [27–29]. However, search within a reduced basis like CRAB has predominantly been implemented using gradient free methods within QOC. In this paper we introduce a method that does derivative-based optimization in a reduced basis called GRAdient Optimization Using Parametrization (GROUP). This method can be understood as combining of CRAB and GRAPE.

All these optimization algorithms are local "hill climber" type searches so depending on their initial seed they will converge towards an optimal solutions or be trapped in a local extremum. As we will demonstrate in this paper, different local algorithms can achieve different results even if they start from the same location. Not only can the results differ, but also the rate of convergence can be very different.

* sherson@phys.au.dk

Derivative-based methods generally converge faster than derivative-free [30]. Derivative-based methods typically employ either steepest-descent or the quasi-Newton method Broyden-Fletcher-Goldfarb-Shanno (BFGS) [30]. BFGS is typically faster than steepest-descent since it avoids steepest-descent's characteristic inefficient zig-zag motion close to the optimum [30]. BFGS achieves this by gradually building an approximation of the Hessian using the past gradients [30]. A graphical illustration of the difference in convergence rate between a derivative free Nelder-Mead and the two derivative based methods is given in Fig. 1.

As mentioned above, for complex optimization landscape topologies local search can fail to find optimal solutions simply due to an unsuccessful seeding strategy [31]. Recent studies have demonstrated that this occurs in constrained quantum control problems [31, 32]. Strong constraints on the total time available (duration) occurs naturally, when seeking the fastest possible solution to some quantum control task (The Quantum Speed Limit) [31, 33].

To investigate the performance of the GROUP algorithm we will compare it to state-of-the-art quantum control algorithms being Krotov's method, Nelder-Mead using CRAB, and GRAPE. We find that GROUP not only converges faster but also achieves better end fidelity. This work supplements and extends on previous efforts in comparing QOC algorithms [34, 35].

We test the algorithms in the context of quantum optimal control for a Bose-Einstein condensate (BEC) manipulated in a magnetic microtrap. These systems are particularly challenging to control due to the non-linearity in the equations of motion. We will investigate fast excitation from the ground state to the first excited state in a single well. This system has attracted much attention in QOC and it has been investigated both experimentally and theoretically [12, 28, 34, 36]. Due to the interest in this system, we see it as an ideal test bed for quantum control algorithms.

This paper is organized as follows. In section II we introduce the control problem of transferring a BEC from the ground state to the first excited state. In section III we present the GROUP methodology and the other different quantum control algorithms. In section IV we compare the different algorithms. Finally, we conclude the paper in section V.

II. THE CONTROL PROBLEM

Here we will discuss the manipulation of a BEC trapped in an atom chip [4]. In the experiment described in Refs. [4, 36] a source for the stimulated emission of matter-waves in twin beams is created by transferring a BEC into the collective first excited state. The typical decay rate of the system is 3 ms, so it is very important to find optimal controls that can transfer the system into the excited state faster than this decay rate and

still allow time for subsequent experiments [4, 28]. This condensate driving (CD) control problem has been investigated using a number of different QOC algorithms in Refs. [12, 28, 34].

In CD, the dynamics are well described by the one-dimensional Gross-Pitaevskii Equation (GPE),

$$i\frac{\partial\psi}{\partial t} = -\frac{1}{2m}\frac{\partial^2\psi}{\partial t^2} + V(x,u)\psi + \beta|\psi|^2\psi \quad (1)$$

$$= (\hat{H} + \beta|\psi|^2)\psi, \quad (2)$$

where $\hbar = 1$, β is the non-linear self interaction and \hat{H} is the Hamiltonian. We can readily assume the system is one-dimensional since the two other spatial directions can be frozen out [28]. The potential is well described by the polynomial,

$$V(x, u(t)) = p_2(x - u(t))^2 + p_4(x - u(t))^4 + p_6(x - u(t))^6,$$

where the control $u(t)$ is the displacement of the trap. The coefficients are given by $p_2 = 2\pi\hbar \cdot 310/r_0^2 \text{J/m}^2$, $p_4 = 2\pi\hbar \cdot 13.6/r_0^4 \text{J/m}^4$ and $p_6 = -2\pi\hbar \cdot 0.0634/r_0^6 \text{J/m}^6$ with $r_0 = 172 \text{nm}$ [28]. The goal is to transfer the initial state ψ_0 into the target state ψ_t after a duration of T . The initial state is the groundstate for $u(t=0) = 0$ and the target state is the first excited state for $u(t=T) = 0$. Here we select a challenging duration at $T = 1.09 \text{ms}$. The value of the nonlinear coupling constant is $\beta = 2.61\hbar \mu\text{mHz}$ for 700 atoms. This takes corrections from going from the three-dimension to the one-dimensional GPE the nonlinear into account [28, 37].

As mentioned above we discuss a state-to-state problem in this paper. In order to find a control that transfers the initial state the problem is expressed as a minimization of the cost functional $J(u, \psi)$,

$$J(u(t), \psi) = \frac{1}{2}(1 - |\langle\psi_t|\psi(T)\rangle|^2) + \frac{\gamma}{2} \int_0^T \dot{u}(t)^2 dt. \quad (3)$$

In the first term $F = |\langle\psi_t|\psi(T)\rangle|^2$ is the fidelity and $1 - F$ is the infidelity, which quantifies the difference between the final state and the target state [12, 34, 38, 39]. The second term in Eq. (3) is the regularization that penalizes strong fluctuations in the control, which accounts for the fact that very fast changes cannot be realized experimentally. We found that $\gamma = 1 \cdot 10^{-6}$ gives an acceptable regularization. Here we investigate the control problem at $T = 1.09 \text{ms}$, where the control problem is highly non trivial [28].

III. QUANTUM OPTIMAL CONTROL

In QOC the goal is to minimize the cost functional $J(u, \psi)$ while satisfying the constraints from the GPE. The constraint can be handled using a Lagrange multiplier,

$$\mathcal{L}(\psi, u, \chi) = J + \Re \int_0^T \langle\chi|i\hbar\dot{\psi} - \hat{H}\psi - \beta|\psi|^2\psi\rangle dt, \quad (4)$$

where χ is a generalized Lagrange multiplier [17]. At a local minimum all the three variational derivatives $D_{\delta\chi}\mathcal{L}$, $D_{\delta\psi}\mathcal{L}$ and $D_{\delta u}\mathcal{L}$ are zero. This gives the following optimality equations (see appendix for details),

$$i\dot{\psi} = \hat{H}\psi + \beta|\psi|^2\psi, \quad (5)$$

$$i\dot{\chi} = (\hat{H} + 2\beta|\psi|^2)\chi + \beta\psi^2\chi^*, \quad (6)$$

$$\gamma\ddot{u} = -\Re\left\langle\chi\left|\frac{\partial\hat{H}}{\partial u}\right|\psi\right\rangle, \quad (7)$$

and the boundary conditions associated,

$$\psi(0) = \psi_0, \quad (8)$$

$$i\chi(T) = -\langle\psi_t|\psi(T)\rangle\psi_t, \quad (9)$$

$$u(0) = u_0, \quad u(T) = u_T. \quad (10)$$

Ideally, these equations would be solved analytically, which would directly give the optimal solutions. Unfortunately, in general these coupled equations cannot be solved analytically, so it is necessary to use iterative numerical algorithms [12, 38].

When performing the numerical optimization of the cost functional it is necessary to discretize the control in steps Δt , where Δt is set by the required accuracy when numerically solving the GPE. This means that the control becomes represented by a vector of length $N = \lfloor T/\Delta t \rfloor$. Typically, in GRAPE and Krotov's method the dimension for the optimization (M) is the same as for the simulation $N = M$. However, with a proper change of basis the optimal controls could adequately be described by another basis with much smaller dimension [40]. In this sense setting $N = M$ often introduces too many degrees of freedom for the optimization. In the simulations performed here we have $N \simeq 3500$ whereas by a proper choice of basis we have only $M \simeq 50$. These potential large reductions in the dimension of the optimization problems is the motivation for reduced or chopped basis methods. In recent years CRAB has emerged as an attractive alternative to the conventional QOC methods, since it parametrizes the control in a reduced basis [20, 22, 28, 41].

As mentioned, the main purpose of this paper is to introduce and numerically test the new method GROUP. We first give a brief review of GRAPE and CRAB since GROUP builds on these methods. When discussing these methods one typically works with the reduced cost functional $\hat{J}(u) = J(u, \psi_u)$. Here ψ_u is the unique solution to the GPE, which is found by solving Eq. (2) with $u(t)$ [39]. Our objective is to find the a minimum and preferably the global minimum of $\hat{J}(u)$.

A. GRAPE

A standard approach to minimizing $\hat{J}(u)$ is the GRAPE algorithm [23, 34, 38]. The simplest version of this method is to update the control along the gradient

$$u^{(i+1)} = u^{(i)} - \alpha^{(i)}\nabla\hat{J}(u^{(i)}), \quad i = 0, 1, 2, \dots \quad (11)$$

Here the index i refers to the current iteration. This is the steepest descent method. An appropriate value for α is found using a step-size algorithm, which solves the one-dimensional optimization problem

$$\alpha^{(i)} = \arg\min_{\alpha} \hat{J}\left(u^{(i)} - \alpha^{(i)}\nabla\hat{J}(u^{(i)})\right). \quad (12)$$

Note, that in Eq. (11) the control is updated for all times $0 \leq t \leq T$ at once. This makes GRAPE a concurrent method, which is different from Krotov's method present later where the control is updated sequentially for each time slice.

An important but subtle point is the use of the gradient $\nabla\hat{J}(u^{(i)})$ in Eq. (11). The complication arises from the fact the the gradient is defined in a function space X . In this space the gradient is the unique element such that $(\nabla\hat{J}, \delta u)_X = D_{\delta u}\hat{J}$ for all possible variations δu . Hence, the gradient depends on the choice of the inner product for the function space X . This has already been discussed in a number of Refs. [38, 39]. Specifically, all variations δu should satisfy the boundary condition in Eq. (10), so we have that $\delta u(0) = \delta u(T) = 0$. A choice that will fulfil this requirement is the H^1 -space with the inner-product $(u, v)_{H^1} = \int_0^T \dot{u}\dot{v}dt$. As shown in the appendix, this choice gives the result,

$$\frac{d^2}{dt^2}[\nabla\hat{J}(u)] = \Re\left\langle\chi\left|\frac{\partial\hat{H}}{\partial u}\right|\psi\right\rangle + \gamma\ddot{u} \quad (13)$$

where ψ and χ are the solutions of Eq. (5) and Eq. (6). This is a Poisson equation for the control in time so we can choose the von Neumann boundary conditions $[\nabla\hat{J}(u)](0) = \nabla[\hat{J}(u)](T) = 0$. These conditions imply that any iteration of GRAPE preserves the boundary condition in Eq. (10). As pointed out in a number of Refs. [38, 39] if we had made the canonical choice of $X = L^2$ then the gradient does not vanish at the boundary. In this case the boundary condition must be enforced numerically by simply setting the gradient to be zero at the boundary, which can greatly decrease the performance of the algorithm.

As discussed above the update written in Eq. (11) is the steepest descent algorithm, which is also illustrated in Fig. 1. It can also be improved by using quasi-Newton method like (BFGS). Again special care has to be taken when working in H^1 -space, and we use the matrix free version of L-BFGS described in Ref. [39].

B. CHOPPED BASIS AND CRAB

As mentioned, above, the dimension for the simulation is $N = \lfloor T/\Delta t \rfloor$ due to the discretization. In GRAPE the dimension for the optimization (M) is $N = M$. However, by expanding the control in a proper basis it is possible to substantially reduce the dimension of the optimization

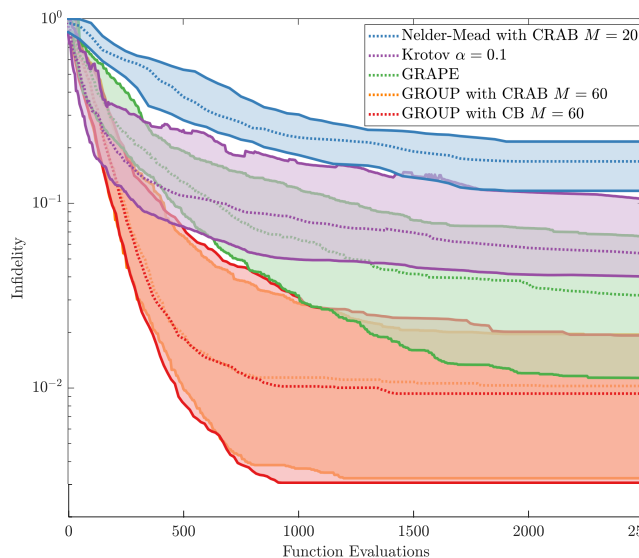


FIG. 2. The infidelity for a given number of function evaluations (solutions of the GPE and Lagrange multiplier Eq. (6)) for the different algorithms. The different algorithms are shown at the basis size or steps size where they performed the best (see legend). The dotted line shows the median and the shaded area indicates the 25%- and 75%-quartiles found from 100 different random initial controls.

problem,

$$u(t) = u_0(t) + S(t) \sum_{n=1}^M c_n f_n(t), \quad (14)$$

where the f_n 's are the basis functions. $S(t)$ is a shape function that enforces the boundary condition in Eq. (10), so we have that $S(0) = S(T) = 0$. In this chopped basis we optimize the coefficients c_n instead of full control $u(t)$, that is, we now optimize the cost function $\hat{J}(\mathbf{c})$ where $\mathbf{c} = (c_1, c_2, \dots, c_M)$. This method is known as a Chopped Basis - CB. The functions f_n must be chosen sensibly based on physical insight, which would typically be sinusoidal functions around characteristic frequencies. The reduced dimension of $\hat{J}(\mathbf{c})$ enables the use of the gradient-free Nelder-Mead algorithm. Gradient-free methods have the advantage that there is no need to implement code that calculates the gradient by solving e.g. Eq. (13), which requires also solving the equation for the Lagrange multiplier (Eq. (6)). This is a particular advantage whenever calculating the gradient is infeasible or too resource consuming [22].

For the control problem discussed here, we found the following expansion useful,

$$u(t) = u_0(t) + S(t) \sum_{n=1}^M c_n \sin\left(\frac{\omega_n t}{T}\right), \quad (15)$$

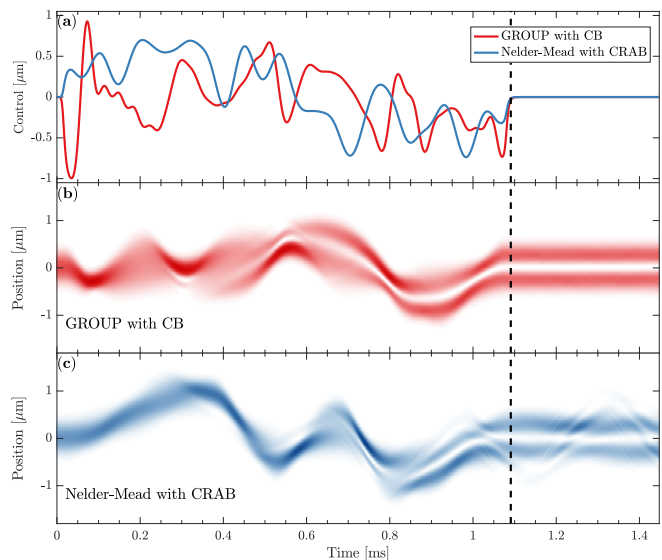


FIG. 3. (a) The best case controls found using GROUP with CB and Nelder-Mead with CRAB shown with red and blue respectively after 2500 iterations. The control is held constant after the vertical dashed line. (b) The density for the condensate ($|\psi(x,t)|^2$) found when using the solution from GROUP. After the vertical line the density is constant, the state has converged with $F = 0.999$ to the first excited state. (c) Here the same is shown as (b) just for Nelder-Mead with CRAB, which has residual oscillations since the final fidelity is $F = 0.92$.

where $\omega_n = n\pi$ is a set of frequencies. This type of chopped basis was extended in Ref. [20] by introducing the Chopped RANdom Basis or CRAB. In CRAB the frequencies ω_n are randomly shifted as $\omega_n = (n+r_n)\pi$ where $-0.5 \leq r_n \leq 0.5$ is an initially chosen random number. The optimization is repeated a number of times with different values of r_n 's. This is a central idea in CRAB, since it allows the algorithm to explore different basis functions with slightly similar frequencies starting from the same u_0 . An optimization within a CRAB can principally be done using any method but it is typically done using the gradient-free method Nelder-Mead [20, 22, 28].

C. GROUP

In GROUP we combine the best features of the two previous methods. We parametrize the control in some basis as in Eq. (14). However, instead of using a gradient-free method to search in the chopped basis we use the gradient descent methods from GRAPE. Here the gradient ($\nabla \hat{J}(\mathbf{c})$) is with respect to the expansion coefficients. Given this gradient an iterative update analogous to Eq. (11) can be directly applied. Just as in GRAPE we need to find an analytic expression for the gradient similar to Eq. (13). The partial derivative of $\hat{J}(u)$ with respect to c_n can be found using the chain-rule for variational derivatives (see

the appendix for more details). The result is

$$\frac{\partial \hat{J}(\mathbf{c})}{\partial c_n} = D_{S(t)f_n(t)} \hat{J}(u) \quad (16)$$

$$= - \int_0^T \left(\Re \left\langle \chi \left| \frac{\partial \hat{H}}{\partial u} \right| \psi \right\rangle + \gamma \ddot{u} \right) S(t) f_n(t) dt. \quad (17)$$

Note that these partial derivatives only differ in the $f_n(t)$ function in the integrand. This expression is valid for any CB and CRAB. The quantity in the bracket need only be computed once, which contains ψ and χ that are found by the numerically expensive solution of Eq. (5)-(6). The cost of calculating all the partial derivatives and hence the full gradient ($\nabla \hat{J}(u)$) is dominated by the solution of Eq. (5)-(6). This implies that the time needed for calculating the gradient in GROUP is comparable to GRAPE.

In the comparative numerical studies presented below we performed the GROUP optimization using the quasi-Newton method BFGS. Note, that when optimizing $\hat{J}(\mathbf{c})$, the optimization is done in the usual l^2 - and not H^1 -space, so all the standard methods for BFGS can be directly applied.

D. Krotov's Method

Krotov's method is an alternative to the standard Lagrange multiplier method used in GRAPE and GROUP [42]. In Krotov's method the cost functional Eq. (3) is rewritten so the GPE appears explicitly and conditions for a guaranteed decrease in the cost are directly built in [24, 25, 34, 42]. This allows Krotov's method to give an optimal control algorithm that directly ensures a monotonic decrease in the cost and it is expected to provide fast convergence. The resulting update for the control is (see appendix for more details)

$$u^{(i+1)}(t) = u^{(i)}(t) + \alpha S(t) \Re \left\langle \chi^{(i)}(t) \left| \frac{\partial \hat{H}}{\partial u} \right|_{u^{(i)}} \right| \psi^{(i+1)}(t) \rangle. \quad (18)$$

Here $\psi^{(i)}$ and $\chi^{(i)}$ are the solutions to the GPE and the Lagrange multiplier from Eq. (5) and Eq. (6) as in GRAPE. $S(t)$ is again a shape function $0 \leq s(t) \leq 1$ that turns the control off at $t = 0$ and $t = T$, which ensures the boundary condition for the control is always satisfied (Eq. (10)). α is the step-size parameter that must be selected for proper convergence. Note that both the current iteration index i and the next index $i + 1$ appears in the equation. Specifically, the control at the next iteration $u^{(i+1)}$ depends on the states in the next iteration $\psi^{(i+1)}$. This makes Krotov's method a sequential algorithm where the next control $u^{(i+1)}$ is being calculated while the equations of motion are being solved along that control. This is very different from the other methods presented here, where the control is updated concurrently for all values of $0 \leq t \leq T$. Note, that since the GPE is nonlinear in the states Eq. (18) should also

include an additional term that is proportional to the difference in the states between iterations [24, 25, 34]. However, this term can be neglected for the small values of β discussed here [34]. Also the derivative is typically with respect to the next iteration ($u^{(i+1)}$), but for the small values of α used here it is acceptable to use the current iteration ($u^{(i)}$) [25, 34].

IV. NUMERICAL RESULTS

In the last section, we gave an introduction to four different quantum control algorithms. In this section, we will compare them numerically when applied on CD. However, before we discuss the results from this numerical study it is necessary to discuss bandwidth limitations on the control.

A. Filter Function

In order to obtain a close match to the experimental conditions in CD it is also necessary to include the finite bandwidth of the control electronics. This effect causes the control $u(t)$ to become distorted into $v(t)$ and the atoms experience the potential from $V(x, v)$ [28]. This effect is large enough to cause the fidelity to drop by a couple of percent, so it must be included in the modelling. The distorted control is given by a convolution with the filter $h(\tau)$

$$v(t) = (h * u)(t) = \int_0^t h(\tau) u(t - \tau) dt. \quad (19)$$

The presence of the filter changes the expressions for the gradients (see the appendix for more details). The GRAPE gradient (Eq. (13)) now becomes

$$\begin{aligned} \frac{d^2}{dt^2} [\nabla \hat{J}(u)] &= -\gamma \dot{v}(T) h(T - t) \\ &+ \int_t^T \left(\Re \left\langle \chi \left| \frac{\partial \hat{H}}{\partial v} \right| \psi \right\rangle + \gamma \ddot{v} \right) dt' \end{aligned} \quad (20)$$

Similarly, the expression for the GROUP gradient becomes

$$\begin{aligned} \frac{\partial \hat{J}(\mathbf{c})}{\partial c_n} &= - \int_0^T \left(\Re \left\langle \chi \left| \frac{\partial \hat{H}}{\partial v} \right| \psi \right\rangle + \gamma \ddot{v} \right) (h * S f_n)(t) dt \\ &+ \gamma \dot{v}(T) (h * S f_n)(T) \end{aligned} \quad (21)$$

It is not straightforward to include such a filter function in Krotov's method. For the comparison below, the simulations for Krotov are performed without the filter. The filter gives rise to another potential complication, which is that although $u(T) = 0$ it can occur that $v(T) \neq 0$. This could slightly perturb the final state, since the control cannot be instantaneously quenched to zero due to the filter. For the optimal solutions found here, this effect did not notably affect the fidelity.

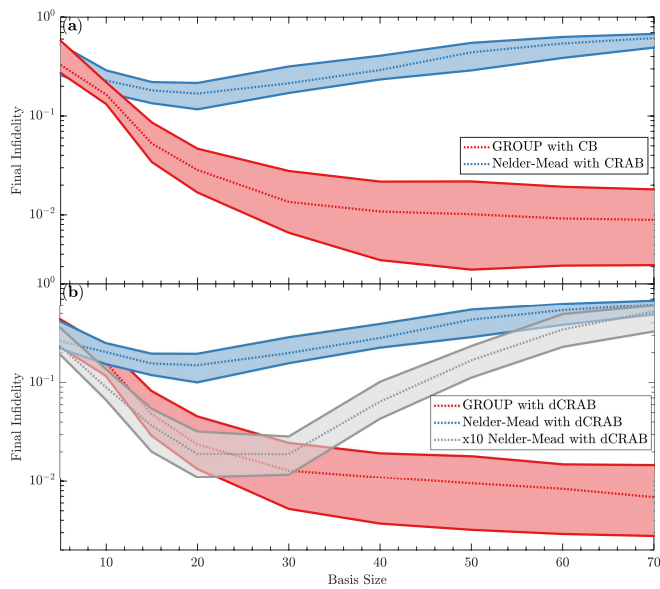


FIG. 4. (a) The final infidelity after 2500 function evaluations for GROUP with CB (red) and Nelder-Mead with CRAB (blue) for different basis sizes. The dotted line is the median and the shaded area display the 25%- and 75%-quartiles found from the 100 different random initial controls. (b) the same as (a) for dressed GROUP and dressed CRAB. The grey plot shows the final infidelity for dressed CRAB after 25,000 iterations rather than 2500 iterations.

B. Convergence Behavior

We applied the following QOC algorithms GRAPE, Krotov, Nelder-Mead using CRAB and GROUP using CB and CRAB to the CD control problem. We applied the algorithms to the same 100 randomly generated initial controls. The convergence behavior of the different methods is illustrated in Fig. 2. Here the median and 25%- and 75%- quartiles are shown for the different algorithms, which gives an impression of the expected behavior for each method on this problem. One function evaluation is a solution of the GPE or the equation for the Lagrange multiplier (Eq. (6)).

Throughout the optimization GROUP achieves the lowest infidelities. At the end of the optimization GROUP has the best infidelity followed by GRAPE and Krotov. There is no particular difference between GROUP using CB or CRAB so we will refer to them both as GROUP. Nelder-Mead using CRAB has the slowest convergence rate of the four methods, since it does not utilize derivative information. This is in accordance with the picture presented in Fig. 1, which shows that derivative-based methods are typically faster than derivative free.

The optimization curves in Fig. 2 can be split into two regimes one at a high number of function evaluations after 600 and one below. Below 600 evaluations GROUP the three derivative based methods have similar rates of convergence. GROUP performs best followed by Krotov and GRAPE. In high number of function evalu-

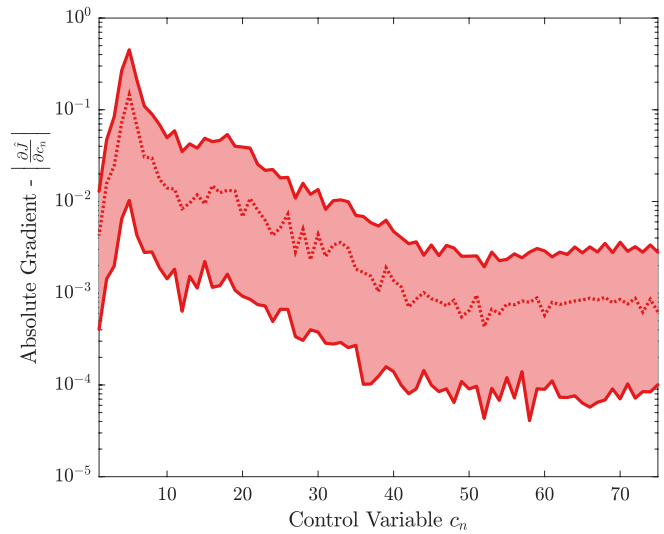


FIG. 5. The absolute value of the partial derivative of the control for the different control coefficients $|\partial \hat{J}(\mathbf{c})/\partial c_n|$ found using Eq. (17). The dotted line shows the median of the 100 gradients taken at the start of the optimization. The shaded area indicate shows the 25%- and 75%-quartiles.

ations regime GROUP performs better than GRAPE and Krotov. We attribute this to the fact that the basis gradually steers GROUP towards a more profitable part of the optimization landscape. This shows the complexity of the optimization landscape, since although the algorithms start at the same point and perform local greedy optimization they converge towards different points with different infidelities. This is different from the situation in Fig. 1 where all the algorithms converge to the same point since the two-dimensional landscape is much simpler than the control problem, which has $M \simeq 3500$ or $M \simeq 50$.

In the high function evaluations regime Krotov and GRAPE switch places and GRAPE finds better infidelities than Krotov. These results show that Krotov achieves a fast initial convergence, but it slows considerably down as it approaches the optimum. GRAPE does not exhibit this behavior, which we attribute to the Hessian approximation from BFGS. BFGS is particularly useful close to the optimum where the objective function can be well described by a second order expansion [30]. Similar results was also reported in Ref. [34]. In principle, Krotov's method can also be combined with a BFGS type method [43]. However, it has been reported in Refs. [34, 43] that this does not significantly improve the convergence.

This comparison focuses on the expected behavior. Each of the methods have a few optimization runs that perform significantly better, which reflects that each algorithm has some specific seeds where it just happens to

search the optimization landscape in the most favorable manner. GROUP had the individual optimization runs with the lowest infidelity. Gradient descent in reduced basis search performed by GROUP is therefore also an advantage when comparing individual best runs.

The best control found for GROUP with CB and Nelder-Mead with CRAB are shown in Fig. 3 with respectively $F = 0.999$ and $F = 0.92$. This figure also shows the density for the condensate when propagated along the optimal controls. After T the control is held constant at $u = 0$. The Nelder-Mead with CRAB solution has a residual oscillation after T , due to residual excited states components in the solution.

C. Reduced Basis Size and Dressed Methods

A limitation of the reduced basis methods is that the optimization might be caught in an artificial trap introduced by limited bandwidth in the parametrization. As an example of this consider our expansion in Eq. (15) at some fixed M . If the optimal solution requires frequencies above M then the optimization can never converge to this solution and it will be caught in an artificial trap. This effect would favor larger values of M . On the other hand, if M is larger then the dimension of the control problem increases, which is exactly what the reduced basis methods attempt to avoid.

In Fig. 4a we compare the trade-off between risk of artificial traps and retaining a low dimension for derivative-free and derivative-based search. As expected a too small basis $M \leq 10$ gives poor results for both algorithms since the optimal controls cannot be adequately described with these small basis sizes. Nelder-Mead with CRAB clearly has an optimal basis size around $M = 20$ and it becomes worse with a larger dimension. This is due to the fact that Nelder-Mead algorithm can no longer effectively search within the large dimension. Surprisingly, the performance in GROUP is very robust with respect to the basis size, it even seems the slightly prefer large basis sizes. We attribute this result to the fact that the large frequencies have small weights in the gradient, and therefore they are not included in the search. This type of behavior is illustrated in Fig. 5, which shows the median initial gradient for the 100 different initial points. Above $n = 50$ the partial derivatives are much smaller than for $n = 5$, hence it is the low frequencies that dominate the search.

A solution to the artificial trap problem was proposed in Ref. [26] where a so-called dressed CRAB (dCRAB) was introduced. In dCRAB the optimization is restarted with new basis functions from the last optimum ($u^{(j-1)}$),

$$u^{(j)} = u^{(j-1)} + \sum_{n=1}^M c_n^{(j)} f_n^{(j)}(t, r_n^{(j)}). \quad (22)$$

These iterations are known as superiterations [26]. The new basis functions $f_n^{(j)}(t, r_n^{(j)})$ are found by reselecting

the random coefficients in CRAB. Hence, this formalism cannot be used in a normal CB. The new basis functions give the algorithm the possibility to escape the artificial traps [26]. This methodology can also be applied to GROUP by simply following the same procedure for the superiterations.

In Fig. 4b we compare the effect of the dressing for different basis sizes. dGROUP does only slightly better than GROUP, which indicates that the solutions were already highly optimal after 2500 evaluations. We observe the same behavior for Nelder-Mead with CRAB after 2500. However, if Nelder-Mead with dCRAB is allowed for run for 25,000 evaluations then it finds much better results especially for basis sizes around $M = 20$. For low basis sizes the results are similar to dGROUP. This shows that if Nelder-Mead runs for much longer times it can find similar results. Nevertheless, due to the slowly improving performance dGROUP finds solutions with the lowest infidelities at larger basis sizes. Simply running Nelder-Mead with CRAB for more evaluations without the dressing does not give this boost to the fidelity. This shows that Nelder-Mead with CRAB was stopped by artificial traps rather than a lack of evaluations. It also shows that the dressing does help CRAB escape artificial traps. On the other hand, for large basis sizes the dressing does not notably improve the infidelity. We interpret this as the optimization being blocked by Nelder-Mead's inability to efficiently search in high dimensional landscapes rather than artificial traps.

V. CONCLUSION & OUTLOOK

We have proposed a QOC algorithm named GROUP that solves state-to-state problems in a reduced basis using gradients. Our strategy combines the advantages from the CRAB and GRAPE methods. We have demonstrated that this algorithm is competitive with other standard methodologies in quantum control by comparing the optimization algorithms on the challenging Condensate Driving problem at $T = 1.09$ ms. We have also included filter effects in modelling, which is not included in most applications within QOC. It would be very interesting to compare these methods on other control problems in order to better understand the advantages and disadvantages of each method. Our optimization strategy can straightforwardly be applied to other quantum control problems such as control of many-body systems [22, 28]. We believe our method is a relevant addition to the repository of quantum control algorithms.

VI. ACKNOWLEDGEMENTS

This work has funded by the European Research Council and the Lundbeck Foundation. We would also like to thank Jesper H. M. Jensen for illuminating discussions and help with adjusting the manuscript. Antonio Ne-

gretti and Marie Bonneau helped with supplying the fil-

ter function and clarifying details in the modelling of the experiment.

-
- [1] I. Bloch, J. Dalibard, and W. Zwerger, *Reviews of modern physics* **80**, 885 (2008).
- [2] R. J. Gordon and S. A. Rice, *Annual review of physical chemistry* **48**, 601 (1997).
- [3] C. Sayrin, I. Dotsenko, X. Zhou, B. Peaudecerf, T. Rybarczyk, S. Gleyzes, P. Rouchon, M. Mirrahimi, H. Amini, M. Brune, *et al.*, *Nature* **477**, 73 (2011).
- [4] R. Bücker, J. Grond, S. Manz, T. Berrada, T. Betz, C. Koller, U. Hohenester, T. Schumm, A. Perrin, and J. Schmiedmayer, *Nature Physics* **7**, 608 (2011).
- [5] B. Bloom, T. Nicholson, J. Williams, S. Campbell, M. Bishof, X. Zhang, W. Zhang, S. Bromley, and J. Ye, *Nature* **506**, 71 (2014).
- [6] B. Lücke, M. Scherer, J. Kruse, L. Pezzé, F. Deuretzbacher, P. Hyllus, J. Peise, W. Ertmer, J. Arlt, L. Santos, *et al.*, *Science* **334**, 773 (2011).
- [7] M. F. Riedel, P. Böhi, Y. Li, T. W. Hänsch, A. Sinatra, and P. Treutlein, *Nature* **464**, 1170 (2012).
- [8] C. Gross, T. Zibold, E. Nicklas, J. Esteve, and M. K. Oberthaler, *Nature* **464**, 1165 (2012).
- [9] I. Bloch, J. Dalibard, and S. Nascimbene, *Nature Physics* **8**, 267 (2012).
- [10] M. Anderlini, P. J. Lee, B. L. Brown, J. Sebby-Strabley, W. D. Phillips, and J. Porto, *Nature* **448**, 452 (2007).
- [11] D. Kielpinski, C. Monroe, and D. J. Wineland, *Nature* **417**, 709 (2002).
- [12] U. Hohenester, P. K. Rekdal, A. Borzi, and J. Schmiedmayer, *Physical Review A* **75**, 023602 (2007).
- [13] J. P. Palao and R. Kosloff, *Physical Review Letters* **89**, 188301 (2002).
- [14] A. Kaiser and V. May, *The Journal of chemical physics* **121**, 2528 (2004).
- [15] S. J. Glaser, U. Boscain, T. Calarco, C. P. Koch, W. Köckenberger, R. Kosloff, I. Kuprov, B. Luy, S. Schirmer, T. Schulte-Herbrüggen, *et al.*, *The European Physical Journal D* **69**, 279 (2015).
- [16] J. Werschnik and E. Gross, *Journal of Physics B: Atomic, Molecular and Optical Physics* **40**, R175 (2007).
- [17] A. P. Peirce, M. A. Dahleh, and H. Rabitz, *Physical Review A* **37**, 4950 (1988).
- [18] C. P. Koch, J. P. Palao, R. Kosloff, and F. Masnou-Seeuws, *Physical Review A* **70**, 013402 (2004).
- [19] T. Nöbauer, A. Angerer, B. Bartels, M. Trupke, S. Rotter, J. Schmiedmayer, F. Mintert, and J. Majer, *Physical review letters* **115**, 190801 (2015).
- [20] T. Caneva, T. Calarco, and S. Montangero, *Physical Review A* **84**, 022326 (2011).
- [21] J. J. W. H. Sørensen, M. Aranburu, T. Heinzl, and J. Sherson, To be published (2018).
- [22] P. Doria, T. Calarco, and S. Montangero, *Physical review letters* **106**, 190501 (2011).
- [23] N. Khaneja, T. Reiss, C. Kehlet, T. Schulte-Herbrüggen, and S. J. Glaser, *Journal of magnetic resonance* **172**, 296 (2005).
- [24] S. E. Sklarz and D. J. Tannor, *Physical Review A* **66**, 053619 (2002).
- [25] D. M. Reich, M. Ndong, and C. P. Koch, *The Journal of chemical physics* **136**, 104103 (2012).
- [26] N. Rach, M. M. Müller, T. Calarco, and S. Montangero, *Physical Review A* **92**, 062343 (2015).
- [27] S. Machnes, D. J. Tannor, F. K. Wilhelm, and E. Assémat, arXiv preprint arXiv:1507.04261 (2015).
- [28] S. van Frank, M. Bonneau, J. Schmiedmayer, S. Hild, C. Gross, M. Cheneau, I. Bloch, T. Pichler, A. Negretti, T. Calarco, *et al.*, *Scientific reports* **6** (2016).
- [29] D. G. Lucarelli, arXiv preprint arXiv:1611.00188 (2016).
- [30] J. Nocedal and S. J. Wright, “Numerical optimization 2nd,” (2006).
- [31] J. J. W. Sørensen, M. K. Pedersen, M. Munch, P. Haikka, J. H. Jensen, T. Planke, M. G. Andreassen, M. Gajdacz, K. Mølmer, A. Lieberoth, *et al.*, *Nature* **532**, 210 (2016).
- [32] D. V. Zhdanov and T. Seideman, *Physical Review A* **92**, 052109 (2015).
- [33] T. Caneva, M. Murphy, T. Calarco, R. Fazio, S. Montangero, V. Giovannetti, and G. E. Santoro, *Physical review letters* **103**, 240501 (2009).
- [34] G. Jäger, D. M. Reich, M. H. Goerz, C. P. Koch, and U. Hohenester, *Physical Review A* **90**, 033628 (2014).
- [35] S. Machnes, U. Sander, S. Glaser, P. de Fouquieres, A. Gruslys, S. Schirmer, and T. Schulte-Herbrüggen, *Physical Review A* **84**, 022305 (2011).
- [36] R. Bücker, T. Berrada, S. Van Frank, J.-F. Schaff, T. Schumm, J. Schmiedmayer, G. Jäger, J. Grond, and U. Hohenester, *Journal of Physics B: Atomic, Molecular and Optical Physics* **46**, 104012 (2013).
- [37] F. Gerbier, *EPL (Europhysics Letters)* **66**, 771 (2004).
- [38] J.-F. Mennemann, D. Matthes, R.-M. Weishäupl, and T. Langen, *New Journal of Physics* **17**, 113027 (2015).
- [39] G. Von Winckel and A. Borzi, *Inverse Problems* **24**, 034007 (2008).
- [40] S. Lloyd and S. Montangero, *Physical review letters* **113**, 010502 (2014).
- [41] I. Brouzos, A. I. Streltsov, A. Negretti, R. S. Said, T. Caneva, S. Montangero, and T. Calarco, *Physical Review A* **92**, 062110 (2015).
- [42] A. Konnov and V. F. Krotov, *Avtomatika i Telemekhanika*, 77 (1999).
- [43] R. Eitan, M. Mundt, and D. J. Tannor, *Physical Review A* **83**, 053426 (2011).
- [44] G. Jäger and U. Hohenester, *Physical Review A* **88**, 035601 (2013).

Appendix: Variations and Gradients

1. Equations of Optimality

Here we give a brief derivation of the optimality equations presented in the main text (Eq. (5)-(10)). The presentation here is based on Refs. [12, 34, 38, 39] In order to find equations for an optimum that also satisfies the GPE we need to calculate the variations with respect to

the Lagrangian

$$\mathcal{L}(\psi, u, \chi) = J(u, \psi) + \Re \int_0^T \langle \chi | Z(u, \psi) \rangle dt, \quad (\text{A.1})$$

where $Z(u, \psi)$ is the constraint given by

$$Z(u, \psi) = i\dot{\psi} - \hat{H}\psi - \beta|\psi|^2\psi. \quad (\text{A.2})$$

Clearly this constraint is zero for any $\psi(t)$ that also satisfies the GPE equation. The optimality system is found by requiring that all first order variations vanish. This

gives us the equations,

$$D_{\delta\chi}\mathcal{L} = D_{\delta\psi}\mathcal{L} = D_{\delta u}\mathcal{L} = 0, \quad (\text{A.3})$$

for all admissible variations. We now calculate these three variations one by one. The variation with respect to χ gives,

$$\begin{aligned} D_{\delta\chi}\mathcal{L} &= D_{\delta\chi}\Re \int_0^T \langle \chi | i\dot{\psi} - \hat{H}\psi - \beta|\psi|^2\psi \rangle dt \\ &= \Re \int_0^T \langle \delta\chi | i\dot{\psi} - \hat{H}\psi - \beta|\psi|^2\psi \rangle dt. \end{aligned}$$

This variation must be zero for all variations $\delta\chi(t)$, which gives Eq. (5). Next consider the variation with respect to ψ . A variation of the constraint gives

$$D_{\delta\psi}\Re \int_0^T \langle \chi | Z \rangle dt = D_{\delta\psi} \left(\Re \langle \chi | i\dot{\psi} \rangle \Big|_0^T - \Re \int_0^T \langle \dot{\chi} | i\psi \rangle dt \right) - \Re \int_0^T \langle \chi | \hat{H}\delta\psi + \beta\psi^2\delta\psi^* + 2\beta|\psi|^2\delta\psi \rangle dt \quad (\text{A.4})$$

$$= \Re \langle i\chi(0) | \delta\psi(0) \rangle - \Re \langle i\chi(T) | \delta\psi(T) \rangle + \Re \int_0^T \langle i\dot{\chi} - \hat{H}\chi - 2\beta|\psi|^2\chi - \beta\psi^2\chi^* | \delta\psi \rangle. \quad (\text{A.5})$$

First consider $0 < t < T$. Since all variations must vanish we find the optimality condition in Eq. (6). For $t = T$ the cost functional $J(u, \psi)$ also contributes with the term

$$D_{\delta\psi}J = -\frac{1}{2}D_{\delta\psi}\langle \psi_t | \psi(T) \rangle \langle \psi(T) | \psi_t \rangle \quad (\text{A.6})$$

$$= -\Re \left(\langle \psi(T) | \psi_t \rangle \langle \psi_t | \delta\psi(T) \rangle \right). \quad (\text{A.7})$$

Combining this Eq. (A.5) gives

$$0 = -\Re \left[\left(\langle i\chi(T) | + \langle \psi(T) | \psi_t \rangle \langle \psi_t | \right) | \delta\psi(T) \right] \quad (\text{A.8})$$

$$+ \Re \langle i\chi(0) | \delta\psi(0) \rangle. \quad (\text{A.9})$$

The first term in this equation gives us the boundary condition for the Lagrange multiplier in Eq. (9). There is also the initial condition that $\psi(0) = \psi_0$ (Eq. (8)), which implies that $\delta\psi(0) = 0$. That means the second term in the equation above is zero. Finally consider the variation with respect to the control u . First, consider the variation with respect the cost functional,

$$D_{\delta u}J = \gamma(\dot{u}(T)\delta u(T) - \dot{u}(0)\delta u(0)) \quad (\text{A.10})$$

$$- \gamma \int_0^T \ddot{u}\delta u dt \quad (\text{A.11})$$

The terms at the boundary vanish, since the control must be fixed at the boundary (Eq. (10)). With this expression, we find the variation of the Lagrangian to be

$$D_{\delta u}\mathcal{L} = - \int_0^T \left(\Re \left\langle \chi \left| \frac{\partial \hat{H}}{\partial u} \right| \psi \right\rangle + \gamma \ddot{u} \right) \delta u dt. \quad (\text{A.12})$$

Since this must vanish for all variation we find the last optimality condition in Eq. (10).

2. Calculation of GRAPE Gradients

In the main text we introduce the gradients for GRAPE. Here we give a brief derivation of these equations. Our considerations follow Refs. [38, 39]. In numerical simulations, we solve the GPE for a given u , so it is more natural to consider the reduced cost functional $\hat{J}(u, \psi) = J(u, \psi_u)$ where ψ_u is the solution to the GPE for a given u . Note that $\hat{J}(u) = \mathcal{L}(\psi_u, u, \chi)$ since $Z(u, \psi_u) = 0$. This is correct for any χ , so χ is a free variable that we can choose conveniently. In order to find the gradient for GRAPE we need the variation of the reduced cost functional

$$D_{\delta u}\hat{J}(u) = D_{\delta u}\mathcal{L}(\psi, u, \chi) + D_{\delta\psi_u}\mathcal{L}(\psi, u, \chi), \quad (\text{A.13})$$

where we have used the total derivative and chain rule. The derivative $D_{\delta\psi_u}\mathcal{L}$ is the induced variation in ψ_u from the variation of u . This extra term appears since ψ depends implicitly on u through the GPE equation. This was not the case when discussing the Lagrangian (Eq. A.1), since ψ is here taken to be a free variable and the GPE is a constraint. Notice that performing this variation is formally the same as the $D_{\delta\psi}$ just with the induced variation instead. Hence, we would get the same equations as above for $D_{\delta\psi}\mathcal{L}$ just with $\delta\psi$ replaced with $\delta\psi_u$. Specifically, we find Eq. (A.5) again for the induced variation. Recall that χ is now a free variable that we can

select. So if we pick χ to satisfy Eq. (6) then the induced variation $D_{\delta\psi_u}$ will vanish. This leads to the conclusion that,

$$D_{\delta u}\hat{J}(u) = D_{\delta u}\mathcal{L}(\psi, u, \chi) \quad (\text{A.14})$$

$$= - \int_0^T \left(\Re \left\langle \chi \left| \frac{\partial \hat{H}}{\partial u} \right| \psi \right\rangle + \gamma \ddot{u} \right) \delta u dt, \quad (\text{A.15})$$

where we have used the result from Eq. (A.12). Recall from the discussion in the main text that the GRAPE gradient is defined as the unique element such that $(\nabla \hat{J}, \delta u)_X = D_{\delta u}\hat{J}$. The gradient depends on the choice of the inner product. The typical choice of the L^2 inner product gives

$$(\nabla \hat{J}, \delta u)_{L^2} = \int_0^T \nabla \hat{J} \delta u dt \quad (\text{A.16})$$

$$= - \int_0^T \left(\Re \left\langle \chi \left| \frac{\partial \hat{H}}{\partial u} \right| \psi \right\rangle + \gamma \ddot{u} \right) \delta u dt. \quad (\text{A.17})$$

From this equation we can immediately recognize that

$$\nabla \hat{J} = -\Re \left\langle \chi \left| \frac{\partial \hat{H}}{\partial u} \right| \psi \right\rangle - \gamma \ddot{u}. \quad \text{for } L^2. \quad (\text{A.18})$$

Note, that there is no reason for this expression to vanish at the boundaries ($t = 0$ and $t = T$). As discussed in the main text failing to satisfy the boundary conditions for the control (Eq. (10)) can cause instabilities in the algorithm. It turns out that a more suitable choice is the H^1 inner product. Here the gradient is

$$(\nabla \hat{J}, \delta u)_{H^1} = \delta u \frac{d}{dt} \nabla \hat{J} \Big|_0^T - \int_0^T \delta u \frac{d^2}{dt^2} \nabla \hat{J} dt \quad (\text{A.19})$$

$$= - \int_0^T \left(\Re \left\langle \chi \left| \frac{\partial \hat{H}}{\partial u} \right| \psi \right\rangle + \gamma \ddot{u} \right) \delta u dt.$$

The first term in Eq. (A.19) vanishes since $\delta u(0) = \delta u(T) = 0$. From this expression we can directly read off the H^1 gradient

$$\frac{d^2}{dt^2} [\nabla \hat{J}(u)] = \gamma \ddot{u} + \Re \left\langle \chi \left| \frac{\partial \hat{H}}{\partial u} \right| \psi \right\rangle \quad \text{for } H^1. \quad (\text{A.20})$$

which is the result given in Eq. (13). This is a Poisson equation, so the von Neumann boundary condition that the gradients vanish at the boundaries can be chosen. This is the motivation for using the H^1 gradient over the L^2 gradient.

As discussed in the main text, it is necessary in CD to take the finite bandwidth of the electronics into account. This effect distorts the control $u(t)$ into $v(t)$, which enters into the GPE equation. This can be modelled using a filter function $h(t)$,

$$v(t) = (h * u)(t) = \int_0^t h(\tau) u(t - \tau) dt, \quad (\text{A.21})$$

where $v(t)$ is the distorted control. Again, we can calculate the variation. This can be done with the chain rule for variations,

$$D_{\delta u}\hat{J}(v) = D_{D_{\delta v}}\hat{J}(v) \quad (\text{A.22})$$

$$= - \int_0^T \left(\Re \left\langle \chi \left| \frac{\partial \hat{H}}{\partial v} \right| \psi \right\rangle + \gamma \ddot{v} \right) (h * \delta u)(t) dt. \quad (\text{A.23})$$

The first term is directly found from Eq. (A.12) where the expression inside the bracket is evaluated along the distorted control $v(t)$. Note that when calculating the variation of the regularization with respect to u , two boundary terms were zero due to the boundary conditions for δu . However, the first of these terms is not zero when filter is included. This gives the second term in the equation above. This equation can be rewritten as

$$D_{\delta u}\hat{J}(v) = - \int_0^T \delta u(t) \left[\gamma \dot{v}(T) h(T - t) - \left(\Re \left\langle \chi \left| \frac{\partial \hat{H}}{\partial v} \right| \psi \right\rangle + \gamma \ddot{v} \right) \Theta(t' - t) dt' \right] dt,$$

where $\Theta(t' - t)$ is the Heaviside-step function. From this expression we can identify the gradients for both L^2 and H^1 . A similar expression for the filter gradient was reported in Ref. [44]. With the same arguments as in Eq. (A.19) the H^1 gradient is given as

$$\frac{d^2}{dt^2} [\nabla \hat{J}(u)] = -\gamma \dot{v}(T) h(T - t) \quad (\text{A.24})$$

$$+ \int_t^T \left(\Re \left\langle \chi \left| \frac{\partial \hat{H}}{\partial v} \right| \psi \right\rangle + \gamma \ddot{v} \right) dt' \quad (\text{A.25})$$

This is the expression given in the main text.

3. Calculation of GROUP Gradients

Here we give a brief deviation of the GROUP gradient expression presented in the main text. As discussed in the main text in GROUP the control is expressed as the linear combination

$$u(t) = u_0(t) + S(t) \sum_{n=1}^M c_n f_n(t), \quad (\text{A.26})$$

where the $f_n(t)$ are smooth functions. Here the optimization is over the expansion coefficients c_n 's. The partial derivative with respect to one of these coefficients can be found using the chain-rule for variational derivatives

$$\frac{\partial \hat{J}(\mathbf{c})}{\partial c_n} = D_{S(t)f_n(t)}\hat{J}(u) \quad (\text{A.27})$$

$$= - \int_0^T \left(\Re \left\langle \chi \left| \frac{\partial \hat{H}}{\partial u} \right| \psi \right\rangle + \gamma \ddot{u} \right) S(t) f_n(t) dt, \quad (\text{A.28})$$

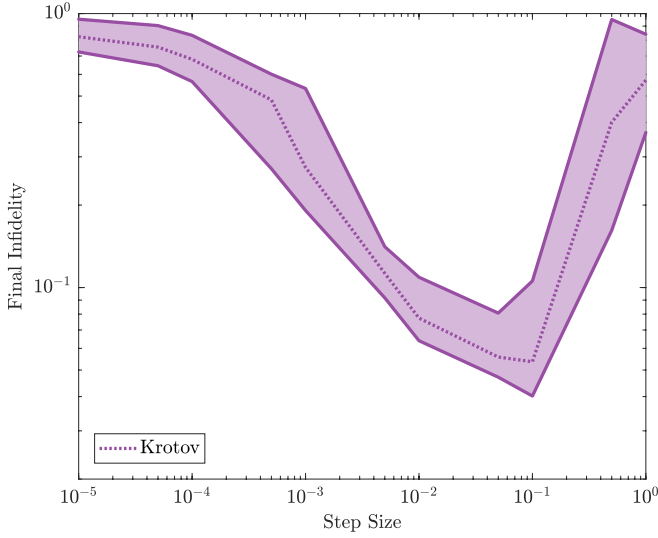


FIG. 6. The final infidelity after 2500 evaluations for Krotov as a function of the step size (α) used in eq. (18). The dotted line and shaded area shows the median, 25%- and 75%-quartiles for the 100 initial controls.

where we have simply reused the result from Eq. (A.12) and replaced $\delta u(t)$ with $S(t)f_n(t)$. There is no contribution from the boundary terms in the regularization since $S(0) = S(T) = 0$. This chain-rule also allows us to take the filter function into account, since we can perform the same substitution with $\delta u(t)$ for $S(t)f_n(t)$ just using the expression in Eq. (A.23)

$$\frac{\partial \hat{J}(v)}{\partial c_n} = - \int_0^T \left(\Re \left\langle \chi \left| \frac{\partial \hat{H}}{\partial v} \right| \psi \right\rangle + \gamma \ddot{v} \right) (h * S f_n)(t) dt + \gamma \dot{v}(T) (h * S f_n)(T) \quad (\text{A.29})$$

The expression inside the bracket is evaluated along the distorted control $v(t)$.

4. Krotov's Method

As discussed in the main text Krotov's method is an alternative to the Lagrange multiplier approach to derive optimal control algorithms [25, 42]. Here we briefly present Krotov's method as described in Refs. [24, 25, 43]. We do not include the regularization term in Krotov so the cost functional becomes $J_T = (1 - |\langle \psi_t | \psi(T) \rangle|^2)/2$. In Krotov's method the cost functional is rewritten so the GPE appears explicitly. This done by adding the vanishing quantity $0 = \phi(T) - \phi(0) - \int_0^T \frac{d\phi}{dt} dt$. Here ϕ is some arbitrary field, which we can select freely. In order to present the derivation more clearly we write the variational derivatives differently here and adopt the standard notation that $\dot{\psi} = f(\psi, u) = -i\hat{H}_{\text{NL}}\psi$ where \hat{H}_{NL} is the GPE Hamiltonian from Eq. (2). This allows

the cost functional to be rewritten as,

$$L = G(\psi(T) - \phi(0)) - \int_0^T R(\psi, u) dt \quad (\text{A.30})$$

where

$$G(\psi(T)) = J_T + \phi(T), \quad (\text{A.31})$$

$$R(\psi, u) = \frac{\partial \psi}{\partial t} + \frac{\delta \phi}{\delta \psi} f + f^* \frac{\delta \phi}{\delta \psi^*}, \quad (\text{A.32})$$

From the arguments above and the definition of R it is seen that $L = J$ as discussed in Ref. [24]. So minimizing J is equivalent to minimizing L . In Krotov's method it is required directly that the cost decreases at each iteration so $J^{(i+1)} \leq J^{(i)}$, which is equivalent to $0 \leq L^{(i)} - L^{(i+1)} = \Delta_1 + \Delta_2 + \Delta_3$ where,

$$\Delta_1 = G(\psi^{(i)}(T)) - G(\psi^{(i+1)}(T)), \quad (\text{A.33})$$

$$\Delta_2 = \int_0^T R(\psi^{(i+1)}, u^{(i+1)}) - R(\psi^{(i+1)}, u^{(i)}) dt, \quad (\text{A.34})$$

$$\Delta_3 = \int_0^T R(\psi^{(i+1)}, u^{(i)}) - R(\psi^{(i)}, u^{(i)}). \quad (\text{A.35})$$

A sufficient condition for a decrease in the cost is that each of these Δ 's are positive. Central in Krotov's method is the unintuitive notion that L is maximized with respect to the states at the current iteration. This implies that any change in the states caused by selecting a new value of the control for the next iteration would decrease the value of L [24, 25]. If L is maximal with respect to the states, then the first order derivatives with respect to ψ^* must vanish. These derivatives are,

$$\begin{aligned} \frac{\delta R}{\delta \psi^*} &= \left(\frac{\partial}{\partial t} + f \frac{\delta}{\delta \psi} + f^* \frac{\delta}{\delta \psi^*} \right) \frac{\delta \phi}{\delta \psi^*} + \frac{\delta \phi}{\delta \psi} \frac{\delta f}{\delta \psi^*} + \frac{\delta f^*}{\delta \psi^*} \frac{\delta \phi}{\delta \psi^*} \\ &= \frac{d}{dt} \frac{\delta \phi}{\delta \psi^*} + \frac{\delta \phi}{\delta \psi} \frac{\delta f}{\delta \psi^*} + \frac{\delta f^*}{\delta \psi^*} \frac{\delta \phi}{\delta \psi^*}, \end{aligned} \quad (\text{A.36})$$

and

$$\frac{\delta G}{\delta \psi^*} = \frac{\delta J_T}{\delta \psi^*} + \frac{\delta \phi(T)}{\delta \psi^*}. \quad (\text{A.37})$$

From the discussion above we require that $\delta R / \delta \psi^*|_{\psi^{(i)}, u^{(i)}} = 0$ and $\delta G / \delta \psi^*|_{\psi^{(i)}, u^{(i)}} = 0$. This condition gives for R that,

$$\begin{aligned} \frac{d}{dt} \frac{\delta \phi}{\delta \psi^*} \Big|_{\psi^{(i)}, u^{(i)}} &= \left(i\psi \frac{\delta \hat{H}_{\text{NL}}}{\delta \psi^*} \frac{\delta \phi}{\delta \psi} - i\psi^* \frac{\delta \hat{H}_{\text{NL}}}{\delta \psi^*} \frac{\delta \phi}{\delta \psi^*} \right. \\ &\quad \left. - i\hat{H}_{\text{NL}} \frac{\delta \phi}{\delta \psi^*} \right) \Big|_{\psi^{(i)}, u^{(i)}}. \end{aligned} \quad (\text{A.38})$$

The requirement that L is maximal with respect to ψ also puts requirements on the second order derivatives of R and G . A good ansatz for ϕ is a second order expansion in the states

$$\phi = \frac{1}{2} \left(\langle \xi | \psi \rangle + \langle \psi | \xi \rangle \right) + \frac{1}{4} \langle \Delta \psi | \sigma | \Delta \psi \rangle, \quad (\text{A.39})$$

where ξ are some expansion coefficients, σ is some function, and $\Delta\psi = \psi - \psi^{(i)}$ is the difference from the next iteration to the current. If this expression is inserted in Eq. (A.37) and (A.38) one obtains,

$$i\dot{\xi}^{(i)} = (\hat{H}(u^{(i)}) + 2\beta|\psi^{(i)}|^2)\xi^{(i)} - (\psi^{(i)})^2\beta\xi^{(i)*} \quad (\text{A.40})$$

$$\xi^{(i)}(T) = -|\psi_t\rangle\langle\psi_t|\psi^{(i)}(T)\rangle. \quad (\text{A.41})$$

Incidentally, these equations are the same as those for χ given in Eq. (6) and Eq. (9) with an extra phase factor, so we have $\xi = i\chi$. We now discuss the additional conditions that ensure that each Δ is positive.

The boundary condition for ξ (Eq. (A.41)) can be combined with the definition of G Eq. (A.31), which gives

$$G(\psi(T)) = \frac{1}{2}\left(1 - \langle\psi(T)|\hat{P}|\psi(T)\rangle + \langle\psi^{(i)}(T)|\hat{P}|\psi(T)\rangle + \langle\psi(T)|\hat{P}|\psi^{(i)}(T)\rangle\right), \quad (\text{A.42})$$

where $\hat{P} = |\psi_t\rangle\langle\psi_t|$ is the projection operator for the target state. From this expression Δ_1 can be directly rewritten as $\Delta_1 = \langle\Delta\psi|\hat{P}|\Delta\psi\rangle$, which always non-negative due to the positivity of \hat{P} .

Generally, it is more difficult to ensure that Δ_3 is positive. Additional conditions on the second order derivatives with respect to the states on R are also required e.g. $\delta^2 R/\delta\psi\delta\psi^*|_{\psi^{(i)}} > 0$. This can be ensured with a proper choice of the σ function. A number of different strategies for choosing σ have been discussed in the literature [24, 25, 34]. For the moderate values of β discussed here a good strategy is simply to select $\sigma(t) = 0$ and forfeit the strict guarantee that Δ_3 is positive [34].

Finally, we discuss how to ensure Δ_2 is positive by a proper update for the control. Ideally, we seek a control such that the derivative vanishes ($\partial R/\partial u|_{u^{(i+1)}, \psi^{(i+1)}} =$

0). The derivative is,

$$\begin{aligned} \frac{\partial R}{\partial u}\Big|_{u^{(i+1)}, \psi^{(i+1)}} &= \Im\left[\left\langle\xi\left|\frac{\partial\hat{H}}{\partial u}\right|\psi\right\rangle\right] \\ &+ \frac{\sigma}{2}\left\langle\Delta\psi\left|\frac{\partial\hat{H}}{\partial u}\right|\psi\right\rangle\Big|_{u^{(i+1)}, \psi^{(i+1)}} \end{aligned} \quad (\text{A.43})$$

It is difficult to ensure that this is zero [25]. Instead of choosing the optimal control, we take a small step in the direction of the gradient,

$$u^{(i+1)} = u^{(i)} + \alpha S(t) \frac{\partial R}{\partial u}\Big|_{\psi^{(i+1)}, u^{(i)}}, \quad (\text{A.44})$$

where $\alpha > 0$ and $s(t)$ is the shape function that vanishes for $t = 0$ and $t = T$ so the boundary conditions on the control can be satisfied (Eq. (10)). If $R(\psi^{(i+1)}, u^{(i+1)})$ in Δ_2 is Taylor expanded around the last control we find,

$$\Delta_2 \approx \int_0^T \frac{\partial R}{\partial u}\Big|_{\psi^{(i+1)}, u^{(i)}} (u^{(i+1)} - u^{(i)}) dt \quad (\text{A.45})$$

$$= \int_0^T \alpha \left(\frac{\partial R}{\partial u}\Big|_{\psi^{(i+1)}, u^{(i)}}\right)^2 dt \geq 0 \quad (\text{A.46})$$

These arguments show that if the control is chosen as in Eq. (A.44) then all three Δ 's are positive and the cost will decrease. If Eq. (A.44) is rewritten with χ then Eq. (18) given in the main text is found. Note, that if $\beta = 0$ then R is independent of ψ and $\Delta_3 = 0$. If $\Delta_3 = 0$ we can just pick $\sigma = 0$ and the algorithm is guaranteed to decrease the cost at every iteration.

A proper value of the step size α must also be selected in order to ensure a fast convergence. In Fig. 6. the performance of the Krotov algorithm in CD is shown for different step sizes. The optimal step size is around 0.1. If the step size is too small the the algorithm converges slowly due to the small steps in the update. On the other hand, if the steps are too large then there is no longer a guarantee that Δ_3 is positive and the update might not decrease the cost.